

# Recursive Identification of Hysteresis in Smart Materials

Xiaobo Tan\* and John S. Baras

**Abstract**—This paper studies recursive identification of hysteresis in smart materials. A Preisach operator with a piecewise uniform density function is used to model the hysteresis. Persistent excitation conditions for parameter convergence are discussed in terms of the input to the Preisach operator. Two classes of recursive identification schemes are explored, one based on the hysteresis output, the other based on the time difference of the output. Experimental results based on a magnetostrictive actuator are presented.

## I. INTRODUCTION

Smart materials, e.g., magnetostrictives, piezoelectrics, and shape memory alloys (SMA), exploit strong coupling between applied electromagnetic/thermal fields and strains for actuation and sensing. The ubiquitous presence of hysteresis in smart materials, however, poses a significant challenge for the effective use of these materials in sensors and actuators. To address this problem, a proper mathematical model for the hysteresis is necessary.

Hysteresis models can be roughly classified into physics-based models and phenomenological models. Physics-based models are built based on first principles of physics, an example of which is the Jiles-Atherton model of ferromagnetic hysteresis [1]. Phenomenological models, on the other hand, are used to produce behaviors similar to those of physical systems without necessarily providing physical insight into the problems. The most popular hysteresis model used for smart materials has been the Preisach operator [2], [3], [4], [5], [6], [7], [8], which is of the phenomenological type. A similar type of operator called Krasnosel'skii-Pokrovskii (KP) operator has also been used [9], [10].

Hysteretic behaviors of smart materials often vary with time, temperature and some other ambient conditions. Therefore, online identification of the hysteresis model is of practical interest. The idea of adaptive inverse control was studied for a class of hysteresis models with piecewise linear characteristics in [11], where the hysteresis parameters (and the inverse hysteresis model) are updated recursively. More recently, similar ideas were applied to control of hysteresis in smart materials [12], [13], where the KP operator and the Prandtl-Ishlinskii operator were used as the hysteresis model, respectively.

This research was supported by the Army Research Office under the ODDR&E MURI97 Program Grant No. DAAG55-97-1-0114 to the Center for Dynamics and Control of Smart Structures (through Harvard University) and by the Lockheed Martin Chair Endowment Funds.

\* Corresponding author. X. Tan is with the Institute for Systems Research, University of Maryland, College Park, MD 20742, USA [xb-tan@umd.edu](mailto:xb-tan@umd.edu)

J. S. Baras is with the Institute for Systems Research and the Department of Electrical & Computer Engineering, University of Maryland, College Park, MD 20742, USA [baras@isr.umd.edu](mailto:baras@isr.umd.edu)

This paper deals with recursive identification of the Preisach operator. Two classes of identification schemes are explored, one based on the hysteresis output, the other based on the time difference of the output. Persistent excitation (P.E.) conditions for parameter convergence are studied in terms of the input to the hysteresis operator. Practical issues in implementation are also discussed. Experimental results based on a magnetostrictive actuator, together with simulation results, are presented.

The remainder of the paper is organized as follows. The Preisach operator is briefly reviewed in Section II, where a discretization scheme is also included. Recursive identification algorithms are presented in Section III. Persistent excitation conditions are discussed in Section IV. Simulation and experimental results are reported in Section V. Finally some conclusions are provided in Section VI.

## II. THE PREISACH OPERATOR

The Preisach operator is briefly reviewed in this section. A more detailed treatment can be found in [14], [15]. A basic element of the Preisach operator is a delayed relay with a pair of switching thresholds  $(\beta, \alpha)$ , as illustrated in Fig. 1. Such an element is called a *hysteron*, and is denoted here by  $\hat{\gamma}_{\beta, \alpha}$ . Let  $C([0, T])$  denote the space of continuous functions on  $[0, T]$ . For  $u \in C([0, T])$  and an initial configuration  $\zeta \in \{-1, 1\}$ , the output of the hysteron is denoted as  $\omega(t) = \hat{\gamma}_{\beta, \alpha}[u, \zeta](t), \forall t \in [0, T]$ .

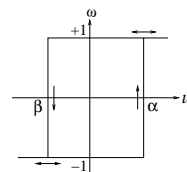


Fig. 1. An elementary hysteron  $\hat{\gamma}_{\beta, \alpha}[\cdot, \cdot]$ .

The Preisach operator is a weighted superposition of all possible hysterons. Define  $\mathcal{P}_0 \triangleq \{(\beta, \alpha) \in \mathbb{R}^2 : \beta \leq \alpha\}$ .  $\mathcal{P}_0$  is called the *Preisach plane*, and each  $(\beta, \alpha) \in \mathcal{P}_0$  is identified with the hysteron  $\hat{\gamma}_{\beta, \alpha}$ . For  $u \in C([0, T])$  and an initial configuration  $\zeta_0$  of all hysterons,  $\zeta_0 : \mathcal{P}_0 \rightarrow \{-1, 1\}$ , the output of the Preisach operator  $\Gamma$  is defined as:

$$y(t) = \Gamma[u, \zeta_0](t) = \int_{\mathcal{P}_0} \mu(\beta, \alpha) \hat{\gamma}_{\beta, \alpha}[u, \zeta_0(\beta, \alpha)](t) d\beta d\alpha, \quad (1)$$

where the weighting function  $\mu(\cdot, \cdot)$  is called the Preisach density function. It is assumed that  $\mu \geq 0$ . Furthermore, to simplify the discussion, assume that  $\mu$  has a compact support, i.e.,  $\mu(\beta, \alpha) = 0$  if  $\beta < \beta_0$  or  $\alpha > \alpha_0$  for some

$\beta_0, \alpha_0$ . In this case it suffices to consider a finite triangular area  $\mathcal{P} \triangleq \{(\beta, \alpha) \in \mathcal{P}_0 | \beta \geq \beta_0, \alpha \leq \alpha_0\}$ , and  $\mathcal{P}$  will also be called the Preisach plane when no confusion arises.

At any time  $t$ ,  $\mathcal{P}$  can be divided into two regions:

$$\begin{aligned} \mathcal{P}_+(t) &\triangleq \{(\beta, \alpha) \in \mathcal{P} | \text{output of } \hat{\gamma}_{\beta, \alpha} \text{ at } t \text{ is } +1\}, \\ \mathcal{P}_-(t) &\triangleq \{(\beta, \alpha) \in \mathcal{P} | \text{output of } \hat{\gamma}_{\beta, \alpha} \text{ at } t \text{ is } -1\}. \end{aligned}$$

Under mild conditions, each of  $\mathcal{P}_+(t)$  and  $\mathcal{P}_-(t)$  is a connected set, and the boundary between them, called *the memory curve*, characterizes the memory of the Preisach operator.

In identification of the Preisach density a discretization step is involved in one way or another (see [16] for a review of identification methods). One discretization scheme is to divide the input range into  $L$  intervals uniformly (called *discretization of level  $L$* ), which results in a discretization grid on the Preisach plane. Denote the discrete input levels by  $u_i$ ,  $1 \leq i \leq L+1$ , i.e.,

$$u_i = u_{min} + (i-1)\Delta_u,$$

where  $\Delta_u = \frac{u_{max} - u_{min}}{L}$ . The cells in the discretization grid are labeled, as illustrated in Fig 2(a) for the case of  $L = 4$ .

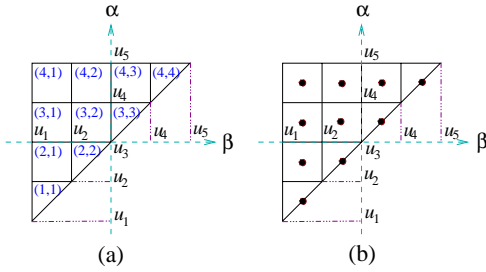


Fig. 2. Illustration of the discretization scheme ( $L = 4$ ): (a) Labeling of the discretization cells; (b) Weighting masses sitting at the centers of cells.

A natural way to approximate a Preisach operator is to assume that inside each cell of the discretized Preisach plane, the Preisach density function is constant. Note that such an operator is still an infinite-dimensional operator. If one assumes that the Preisach weighting function inside each cell is concentrated at the center as a weighting mass (Fig. 2(b)), the corresponding Preisach operator becomes a weighted combination of a finite number of hysterons. Equivalently the input takes values in the finite set  $\{u_i\}_{i=1}^{L+1}$ .

### III. RECURSIVE IDENTIFICATION SCHEMES

The discrete-time setting is considered in this paper. A Preisach operator with discrete weighting masses is easier to analyze than a Preisach operator with a piecewise uniform weighting density; however, these two types of operators bear much similarity and essential results for one can be easily translated into those for the other. Hence recursive identification of Preisach weighting masses is first studied, and then the extension needed for identifying the density directly is briefly discussed.

In this paper two classes of identification algorithms are examined, one based on the hysteresis output, and the other based on the time difference of the output (called *difference-based* hereafter).

*Output-based identification:* The output  $y[n]$  of the discretized Preisach operator (corresponding to the case illustrated in Fig. 2(b)) at time instant  $n$  can be expressed as

$$y[n] = \sum_{i=1}^L \sum_{j=1}^i \bar{W}_{ij}[n] \bar{\nu}_{ij}^*, \quad (2)$$

where  $\bar{W}_{ij}[n]$  denotes the state (1 or -1) of the hysteron in cell  $(i, j)$  at time  $n$ , and  $\bar{\nu}_{ij}^*$  denotes the hysteron's Preisach weighting mass. Stacking  $\bar{W}_{i,j}[n]$  and  $\bar{\nu}_{i,j}^*$  into two vectors,  $W[n] = [W_1[n] \cdots W_K[n]]^T$  and  $\nu^* = [\nu_1^* \cdots \nu_K^*]^T$ , where  $K = \frac{L(L+1)}{2}$  is the number of cells, one rewrites (2) as

$$y[n] = \sum_{k=1}^K W_k[n] \nu_k^* = W[n]^T \nu^*. \quad (3)$$

Let  $\hat{\nu}[n] = [\hat{\nu}_1[n] \cdots \hat{\nu}_K[n]]^T$  be the estimate of  $\nu^*$  at time  $n$ , and let

$$\hat{y}[n] = \sum_{k=1}^K W_k[n] \hat{\nu}_k[n] = W[n]^T \hat{\nu}[n] \quad (4)$$

be the predicted output based on the parameter estimate at time  $n$ . The gradient algorithm [17] to update the estimate is

$$\hat{\nu}[n+1] = \hat{\nu}[n] - \gamma \frac{(\hat{y}[n] - y[n])W[n]}{W[n]^T W[n]}, \quad (5)$$

where  $0 < \gamma < 2$  is the adaptation constant. To ensure that the weighting masses are nonnegative, let  $\hat{\nu}_k[n+1] = 0$  if the  $k$ -th component of the right hand side of (5) is negative.

*Difference-based identification:* An alternate way to identify  $\nu^*$  is using the time difference  $z[n]$  of the output  $y[n]$ , where

$$z[n] \triangleq y[n] - y[n-1] = (W[n] - W[n-1])^T \nu^*. \quad (6)$$

Let  $\hat{y}[n^-]$  and  $\hat{y}[n-1]$  be the output predictions at time  $n$  and  $n-1$  based on  $\hat{\nu}[n-1]$ , respectively, i.e.,

$$\hat{y}[n^-] \triangleq W[n]^T \hat{\nu}[n-1], \quad \hat{y}[n-1] \triangleq W[n-1]^T \hat{\nu}[n-1].$$

Define

$$\hat{z}[n] \triangleq \hat{y}[n^-] - \hat{y}[n-1] = (W[n] - W[n-1])^T \hat{\nu}[n-1]. \quad (7)$$

Let  $V[n]$  be the time difference of hysteron states,  $V[n] \triangleq W[n] - W[n-1]$ . Then one can obtain the following identification scheme based on  $z[n]$ :

$$\hat{\nu}[n+1] = \begin{cases} \hat{\nu}[n] - \gamma \frac{z[n] - \hat{z}[n] V[n]}{V[n]^T V[n]}, & \text{if } V[n] \neq 0 \\ \hat{\nu}[n] & \text{if } V[n] = 0 \end{cases}. \quad (8)$$

As in the output-based scheme, an parameter projection step will be applied if any component of  $\hat{\nu}[n+1]$  is negative.

Having discussed the methods for recursive identification of weighting masses for a Preisach operator, we now point

out how to change the previous algorithms for identification of the (piecewise uniform) Preisach density. In this case, the output  $y[n]$  can still be expressed as (2) or (3), but with different interpretations for  $\bar{W}_{i,j}[n]$  and  $\bar{\nu}_{i,j}^*$ . Each component  $\bar{W}_{i,j}[n]$  of  $W[n]$  no longer represents the state (1 or  $-1$ ) of the hysteron at the center of the cell  $(i, j)$ ; instead it represents the *signed area* of the cell:

$$\bar{W}_{i,j}[n] = \text{area of } C_{i,j}^+[n] - \text{area of } C_{i,j}^-[n],$$

where  $C_{i,j}^+$  ( $C_{i,j}^-$ , resp.) denotes the portion of cell  $(i, j)$  occupied by positive (negative, resp.) hysterons. Each component  $\bar{\nu}_{i,j}^*$  of  $\nu^*$  now represents the true density value on the cell  $(i, j)$ . Similarly,  $\hat{\nu}[n]$  is now the vector of density values estimated at time  $n$ . Define  $V[n] \triangleq W[n] - W[n-1]$ . Define  $\hat{y}[n]$ ,  $z[n]$ , and  $\hat{z}[n]$  as in (4), (6), (7), respectively. Based on these definitions, the output-based algorithm (5) and the difference-based algorithm (8) can be applied without modification to identify  $\nu^*$ .

#### IV. PERSISTENT EXCITATION CONDITIONS

Define the parameter error  $\tilde{\nu}[n] \triangleq \hat{\nu}[n] - \nu^*$ . Then for the output-based algorithm (5) (letting  $\gamma = 1$  without loss of generality),

$$\tilde{\nu}[n+1] = F[n]\tilde{\nu}[n], \quad (9)$$

where  $F[n] = \mathbb{I}_K - \frac{W[n]W[n]^T}{W[n]^T W[n]}$ , and  $\mathbb{I}_K$  represents the identity matrix of dimension  $K$ . It is well-known [17] that the convergence of the algorithm (5) depends on the *persistent excitation* (P.E.) condition of the sequence  $W[n]$ . The sequence  $W[n]$  is persistently exciting if, there exist an integer  $N > 0$  and  $c'_1 > 0, c'_2 > 0$ , such that for any  $n_0$ ,

$$c'_1 \mathbb{I}_K \leq \sum_{n=n_0}^{n_0+N-1} \frac{W[n]W[n]^T}{W[n]^T W[n]} \leq c'_2 \mathbb{I}_K. \quad (10)$$

Due to the equivalence of uniform complete observability under feedback [17], [18], from (10), there exist  $c_1 > 0, c_2 > 0$  such that for any  $n_0$ ,

$$c_1 \mathbb{I}_K \leq G_N(n_0) \leq c_2 \mathbb{I}_K, \quad (11)$$

where  $G_N(n_0)$  is the observability grammian of the system (9) defined as

$$G_N(n_0) = \sum_{n=n_0}^{n_0+N-1} \frac{\Phi[n, n_0]^T W[n] W[n]^T \Phi[n, n_0]}{W[n]^T W[n]},$$

and  $\Phi[n, n_0]$  is the state transition matrix,  $\Phi[n, n_0] = \prod_{k=n_0}^{n-1} F[k]$ . It can be shown [17] that when (11) is satisfied,

$$\|\tilde{\nu}[n+N]\| \leq \sqrt{1-c_1} \|\tilde{\nu}[n]\|, \quad (12)$$

from which exponential convergence to  $\nu^*$  can be concluded. Similarly one can write down the error dynamics equation, the P.E. condition on  $V[n]$ , and the convergence rate estimate for the difference-based scheme (8).

The sequences  $V[n]$  and  $W[n]$  are almost equivalent in the sense that, for any  $N > 0$ ,  $\{V[n]\}_{n=1}^N$  can be constructed from  $\{W[n]\}_{n=0}^N$ , and conversely,  $\{W[n]\}_{n=1}^N$  can be constructed from  $W[0]$  and  $\{V[n]\}_{n=1}^N$ . However, there are motivations to introduce the difference-based scheme (8). For ease of discussion, consider the case of identifying Preisach weighting masses (corresponding to Fig. 2(b)). In this case while  $W[n]$  has components  $\pm 1$ , the components of  $V[n]$  are  $\pm 2$  or 0. Often times most components of  $V[n]$  are 0 since  $V_k[n] \neq 0$  only if the  $k$ -th hysteron changed its state at time  $n$ . This has two consequences: (1) The P.E. condition of  $V[n]$  is easier to analyze than that of  $W[n]$ ; (2) The convergence of the difference-based scheme (assuming that P.E. is satisfied) is expected to be faster than that of the output-based scheme since  $z[n]$  carries more specific information about  $\nu^*$ .

It is of practical interest to express the P.E. conditions in terms of the input  $u[n]$  to the hysteresis operator. The P.E. condition for the difference-based algorithm is equivalent to that  $\{V[n]\}_{n=n_0}^{n_0+N-1}$  spans  $\mathbb{R}^K$  since  $V[n]$  can take only a finite number of possible values. Recall that  $u[n]$  takes values in a finite set  $\{u_i, 1 \leq i \leq L+1\}$ . In the analysis below it is assumed that the input does not change more than one level during one sampling time. The assumption is not restrictive considering the rate-independence [15] of the Preisach operator, but it helps to ease the presentation.

*Theorem 4.1 (Necessary condition for P.E.):* If  $\{V[n]\}$  is P.E., then there exists  $N > 0$ , such that for any  $n_0$ , for any  $i \in \{1, 2, \dots, L\}$ ,  $u[n]$  achieves a local maximum at  $u_{i+1}$  or a local minimum at  $u_i$  during the time period  $[n_0, n_0 + N - 1]$ .

*Proof.* Let us call a hysteron *active* at time  $n$  if it changes state at time  $n$ . Since the input changes at most one level each time, if  $u[n] > u[n-1]$ , the set of active hysterons must have the form  $S_{i,j}^+ \triangleq \{(i, j), (i, j+1), \dots, (i, i)\}$  for some  $i, j$  with  $1 \leq i \leq L$  and  $1 \leq j \leq i$  (refer to the labeling scheme in Fig. 2(a)), and the components of  $V[n]$  corresponding to elements of  $S_{i,j}^+$  are 2 and other components equal 0. Similarly, if  $u[n] < u[n-1]$ , the set of active hysterons has the form  $S_{i,j}^- \triangleq \{(j, j), (j+1, j), \dots, (i, j)\}$  for some  $i, j$ , and the components of  $V[n]$  corresponding to elements of  $S_{i,j}^-$  are  $-2$  and other components equal 0.

If, for some  $i'$ ,  $u_{i'+1}$  is not a local maximum and  $u_{i'}$  is not a local minimum,  $S_{i',i'}^+$  or  $S_{i',i'}^-$  will not become the set of active hysterons during  $[n_0, n_0 + N - 1]$ . In particular, when the hysteron  $(i', i')$  changes state from  $-1$  to 1, so does the hysteron  $(i' - 1, i')$ ; and when the hysteron  $(i', i')$  changes state from 1 to  $-1$ , so does the hysteron  $(i', i' + 1)$ . This implies that the contribution to the output from the hysteron  $(i', i')$  cannot be isolated, and hence  $\{V[n]\}_{n=n_0+1}^{n_0+N-1}$  does not span  $\mathbb{R}^K$ .  $\square$

*Remark 4.1:* From Theorem 4.1, for a Preisach operator with discretization level  $L$ , it is necessary that the input  $u[n]$  has  $L$  reversals at different input levels for parameter convergence. This is in analogy to (but remarkably different

from) the result for linear systems, where the input is required to have at least  $n$  frequency components for identification of  $n$  parameters [17], [18].

Theorem 4.1 implies that the input levels  $u_1$  and  $u_{L+1}$  must be visited for P.E. to hold. When the input hits  $u_1$ , all hysterons have output  $-1$  and the Preisach operator is in negative saturation; similarly, when the input hits  $u_{L+1}$ , the Preisach operator is in positive saturation. For either case all the previous memory is “erased” and the operator is “reset”. Starting from these reset points, one can keep track of the memory curve  $\psi[n]$  (the state of the Preisach operator) according to the input  $u[\cdot]$ .

Consider an input sequence  $\{u[n]\}_{n=n_a}^{n_b}$ ,  $n_a < n_b$ . If there exist  $n_1, n_2, n_3$  and  $n_4$  with  $n_a \leq n_1 < n_2 \leq n_3 < n_4 \leq n_b$  such that the memory curve  $\psi[n_1] = \psi[n_3]$  and  $\psi[n_2] = \psi[n_4]$ , one can obtain another input sequence  $\{u'[n]\}_{n=n_a}^{n_b}$  by swapping the section  $\{u[n]\}_{n=n_1}^{n_2}$  with the section  $\{u[n]\}_{n=n_3}^{n_4}$ . We write  $\{u[n]\}_{n=n_a}^{n_b} \stackrel{P.E.}{\equiv} \{u'[n]\}_{n=n_a}^{n_b}$  (called *equivalent in terms of P.E.*) since the two sequences carry same excitation information for the purpose of parameter identification. The set of all input sequences obtained from  $\{u[n]\}_{n=n_a}^{n_b}$  as explained above (with possibly zero or more than one swappings) form the *P.E. equivalence class* of  $\{u[n]\}_{n=n_a}^{n_b}$ , denoted as  $\{\underline{u}[n]\}_{n=n_a}^{n_b}$ . Note that in particular,  $\{u[n]\}_{n=n_a}^{n_b} \in \{\underline{u}[n]\}_{n=n_a}^{n_b}$ . We are now ready to present a sufficient condition for P.E. in terms of the input  $u[n]$ .

**Theorem 4.2 (Sufficient condition for P.E.):** If there exists  $N > 0$ , such that for any  $n_0$ , one can find  $\{u'[n]\}_{n=n_0}^{n_0+N-1} \in \{\underline{u}[n]\}_{n=n_0}^{n_0+N-1}$  satisfying the following: there exist time indices  $n_0 \leq n_a \leq n_1^- < n_1^+ < n_2^- < n_2^+ < \dots < n_i^- < n_i^+ < \dots \leq n_b \leq n_0 + N - 1$  or  $n_0 \leq n_a \leq n_1^+ < n_1^- < n_2^+ < n_2^- < \dots < n_i^+ < n_i^- < \dots \leq n_b \leq n_0 + N - 1$ , such that  $u'[n_i^+]$  is a local maximum and  $u'[n_i^-]$  is a local minimum of  $\{u'[n]\}_{n=n_a}^{n_b}$  for each  $i$ , these local maxima and minima include all input levels  $u_i$ ,  $1 \leq i \leq L + 1$ , and either

(a)  $\{u'[n_i^+]\}$  is non-increasing,  $u'[n_i^+] \geq u'[n]$  for  $n_i^+ < n \leq n_b$ ,  $u'[n_i^+]$  differs from  $u'[n_{i+1}^+]$  by no more than  $\Delta_u$ , and  $\{u'[n_i^-]\}$  is non-decreasing,  $u'[n_i^-] \leq u'[n]$  for  $n_i^- < n \leq n_b$ ,  $u'[n_i^-]$  differs from  $u'[n_{i+1}^-]$  by no more than  $\Delta_u$ ; or

(b)  $\{u'[n_i^+]\}$  is non-decreasing,  $u'[n_i^+] \leq u'[n]$  for  $n_i^+ < n \leq n_b$ ,  $u'[n_i^+]$  differs from  $u'[n_{i+1}^+]$  by no more than  $\Delta_u$ , and  $\{u'[n_i^-]\}$  is non-increasing,  $u'[n_i^-] \geq u'[n]$  for  $n_i^- < n \leq n_b$ ,  $u'[n_i^-]$  differs from  $u'[n_{i+1}^-]$  by no more than  $\Delta_u$ , then  $V[n]$  corresponding to  $u[n]$  is P.E..

*Proof.* Construct a new input sequence  $\{\bar{u}[n]\}_{n=1}^{\bar{n}}$  (for some  $\bar{n} > 1$ ) which achieves the local maxima  $\{u'[n_i^+]\}$  and the local minima  $\{u'[n_i^-]\}$  with the same order as in  $u'[n]$ , but  $\bar{u}[n]$  varies monotonically from a maximum to the next minimum or from a minimum to the next maximum. For such an input, it can be seen through memory curve analysis on the Preisach plane that the corresponding  $\{\bar{V}[n]\}_{n=1}^{\bar{n}}$  spans  $\mathbb{R}^K$ . From the way  $\bar{u}[n]$  is constructed and the

conditions given in the theorem, any vector in  $\{\bar{V}[n]\}_{n=1}^{\bar{n}}$  must also be present in  $\{V'[n]\}_{n=n_0}^{n_0+N-1}$  corresponding to  $u'[n]$ . Hence  $\{V'[n]\}$  is P.E.. Finally P.E. of  $\{V[n]\}$  follows since  $\{u'[n]\}_{n=n_0}^{n_0+N-1}$  belongs to the P.E. equivalence class of  $\{u[n]\}_{n=n_0}^{n_0+N-1}$ .  $\square$

Theorem 4.2 is not conservative, and it covers a wide class of P.E. inputs. For example, it can be easily verified that a (periodic) first order reversal input [14] (see Fig. 3(a) for case  $L = 4$ ), which has been widely used for identification of Preisach density function, and a (periodic) oscillating input with decreasing amplitude (Fig. 3(b) for case  $L = 4$ ) both satisfy the conditions in Theorem 4.2, and are thus P.E.. In these two cases,  $u[n]$  itself satisfies the conditions imposed for  $u'[n]$  in the theorem. Fig. 4 shows an example where one can conclude the P.E. of a periodic  $u[n]$  by inspecting a P.E. equivalent input  $u'[n]$ . Note that Theorem 4.2 does not require  $u[n]$  to be periodic, although periodic examples are chosen here for easy illustration.

The P.E. conditions (Theorems 4.1 and 4.2) can be extended in a straightforward manner (with minor modifications) to the case where a piecewise uniform density function is to be identified.

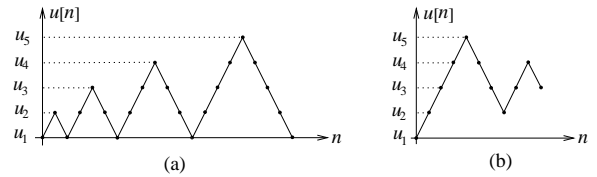


Fig. 3. Examples of P.E. inputs ( $L = 4$ , showing one period): (a) The first order reversal input; (b) An oscillating input with decaying amplitude.

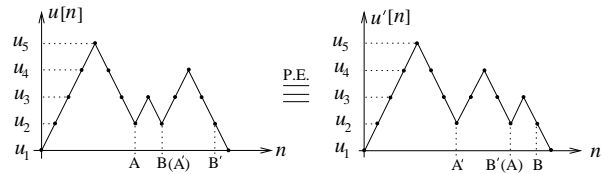


Fig. 4. An example of P.E. input ( $L = 4$ , showing one period). The input  $u'[n]$ , P.E. equivalent to  $u[n]$ , is obtained by swapping two sections  $A - B$  and  $A' - B'$  of  $u[n]$ .

## V. SIMULATION AND EXPERIMENTAL RESULTS

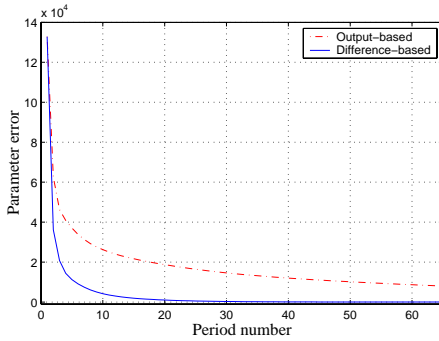
### A. Comparison of the output-based scheme with the difference-based scheme

In this subsection the output-based scheme is compared with the difference-based one through simulation. As shown in (12), the minimum eigenvalue of the observability gram-mian (i.e.,  $c_1$  in (11)) is directly related to the convergence rate of the output-based scheme. The same statement holds for the difference-based scheme provided that  $W[n]$  is replaced with  $V[n]$  in the related equations. In Table I we list the corresponding  $\sqrt{1 - c_1}$  (the bound on the norm of parameter error drop over one period) under the two

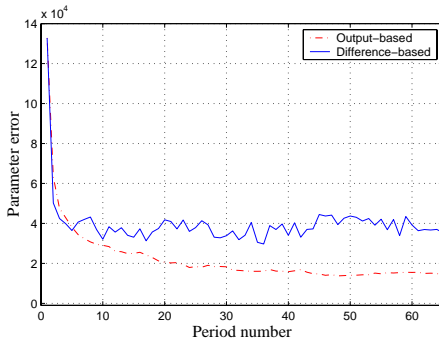
gradient schemes (with  $\gamma = 1$ ) for different discretization levels  $L$  with the (periodic) first order reversal input. From Table I, the difference-based scheme converges faster as expected. Simulation has been conducted for the case  $L = 10$ . Fig. 5(a) compares the decrease of the norm of parameter error over periods when there is no measurement noise, and the conclusion is consistent with Table I.

TABLE I  
COMPARISON OF CONVERGENCE RATES FOR THE OUTPUT-BASED ALGORITHM AND THE DIFFERENCE-BASED ALGORITHM.

$L$	$\sqrt{1 - c_1}$ (Output-based)	$\sqrt{1 - c_1}$ (Difference-based)
5	0.9631	0.9399
10	0.9908	0.9784
15	0.9958	0.9874
20	0.9976	0.9912
25	0.9985	0.9933



(a)



(b)

Fig. 5. Comparison of parameter convergence for the output based algorithm and the difference-based algorithm. (a) Case I: noiseless measurement; (b) Case II: noisy measurement.

Despite the apparent advantage of faster convergence, the difference-based scheme is more sensitive to the measurement noise: the noise gets magnified when one takes the output difference (analogous to taking the derivative of a noisy continuous-time signal), and the disturbance is shared

only among the active hysterons. Simulation in Fig. 5(a) is re-conducted where a noise is added to the output, the noise magnitude being 4% of the saturation output of the Preisach operator. From Fig. 5(b), in this case, the parameter error will not converge to zero under either algorithm. However, the ultimate error of the output-based algorithm is much lower than that of the difference-based scheme.

### B. Experimental results

Experiments have been conducted on a magnetostrictive actuator to examine the identification schemes. The hysteretic relationship between the displacement output of the actuator and its current input can be modeled by a Preisach operator when the current input is quasi-static [7].

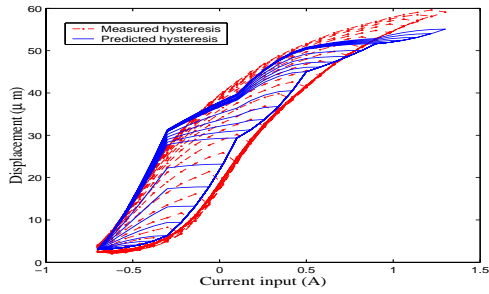
A periodic first order reversal current input is used for recursive identification of the Preisach density function. A practically important issue is the choice of the discretization level  $L$ . Although it is expected that the higher discretization level  $L$ , the higher model accuracy, there are two factors supporting a moderate value of  $L$  in practice: the computational complexity and the sensor accuracy level. Since the number of cells on a discretization grid scales as  $L^2$ , so is the computational complexity of the recursive identification algorithm. It should also be noted that, from Table I, the convergence rate  $\sqrt{1 - c_1}$  decreases as  $L$  increases. Furthermore, in the presence of the sensor noise and unmodeled dynamics, higher discretization level may not necessarily lead to improved performance. Fig. 6 compares the measured hysteresis loops against the predicted loops based on the identified parameters for different  $L$ . Although the scheme with  $L = 10$  achieves much better match than the scheme with  $L = 5$ , there is little improvement when  $L$  is increased to 15. Hence for the particular actuator (and the sensor used), it is determined that  $L = 10$  is an appropriate discretization level. Fig. 7 shows the identified density distribution for  $L = 10$  after eight periods. The output-based gradient algorithm is used with  $\gamma = 1$ .

## VI. CONCLUSIONS

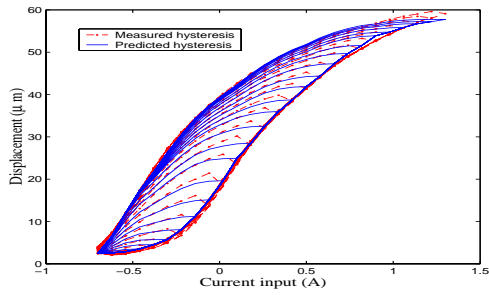
This paper has been focused on recursive identification of hysteresis in smart materials. A Preisach operator with piecewise uniform density function was used to approximate smart material hysteresis. On the theoretical side, a necessary condition and a sufficient condition for the parameter convergence were presented in terms of the input to the Preisach operator. In contrast to the results for linear systems, the conditions here center around the local maxima/minima of the input.

Practical implementation issues were studied through both simulation and experiments. Two types of adaptive gradient identification algorithms were compared. It was found that the difference-based method has a higher convergence rate, but it is more sensitive to the measurement noise. The choice of the level of discretization was also discussed.

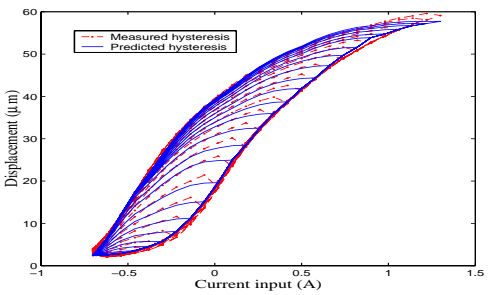
Recently an adaptive inverse control algorithm has been developed using the output-based recursive identification,



(a)



(b)



(c)

Fig. 6. Comparison of measured hysteresis loops with predicted loops based on the identified density. (a)  $L = 5$ ; (b)  $L = 10$ ; (c)  $L = 15$ .

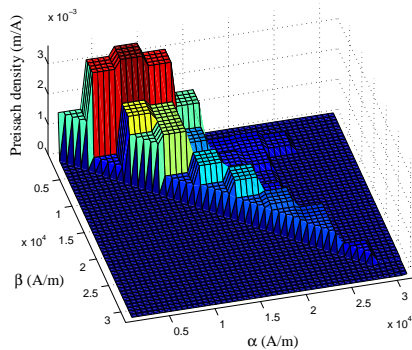


Fig. 7. Identified Preisach density function ( $L = 10$ ).

which will be reported in another paper. For future work, it will be of interest to extend the results here to the cases where the hysteresis output is not directly measurable. Such cases happen if, e.g., the high-frequency dynamics of the smart material actuator is not negligible, or the actuator is used to control some other plant.

## VII. ACKNOWLEDGMENTS

The authors would like to thank the anonymous reviewers for their useful comments.

## REFERENCES

- [1] D. C. Jiles and D. L. Atherton, "Theory of ferromagnetic hysteresis," *Journal of Magnetism and Magnetic Materials*, vol. 61, pp. 48–60, 1986.
- [2] A. A. Adly, I. D. Mayergoyz, and A. Bergqvist, "Preisach modeling of magnetostrictive hysteresis," *Journal of Applied Physics*, vol. 69, no. 8, pp. 5777–5779, 1991.
- [3] D. Hughes and J. T. Wen, "Preisach modeling and compensation for smart material hysteresis," in *Active Materials and Smart Structures*, G. L. Anderson and D. C. Lagoudas, Eds., 1994, vol. 2427 of *SPIE*, pp. 50–64.
- [4] J. Schäfer and H. Janocha, "Compensation of hysteresis in solid-state actuators," *Sensors and Actuators A*, vol. 49, no. 1-2, pp. 97–102, 1995.
- [5] P. Ge and M. Jouaneh, "Tracking control of a piezoceramic actuator," *IEEE Transactions on Control Systems Technology*, vol. 4, no. 3, pp. 209–216, 1996.
- [6] R. B. Gorbet, D. W. L. Wang, and K. A. Morris, "Preisach model identification of a two-wire SMA actuator," in *Proceedings of IEEE International Conference on Robotics and Automation*, 1998, pp. 2161–2167.
- [7] X. Tan, R. Venkataraman, and P. S. Krishnaprasad, "Control of hysteresis: Theory and experimental results," in *Modeling, Signal Processing, and Control in Smart Structures*, V. S. Rao, Ed., 2001, vol. 4326 of *SPIE*, pp. 101–112.
- [8] D. Croft, G. Shed, and S. Devasia, "Creep, hysteresis, and vibration compensation for piezoactuators: atomic force microscopy application," *Journal of Dynamic Systems, Measurement, and Control*, vol. 123, no. 1, pp. 35–43, 2001.
- [9] H. T. Banks, A. J. Kurdila, and G. Webb, "Identification of hysteretic control influence operators representing smart actuators, Part I: Formulation," *Mathematical Problems in Engineering*, vol. 3, no. 4, pp. 287–328, 1997.
- [10] W. S. Galinaitis and R. C. Rogers, "Control of a hysteretic actuator using inverse hysteresis compensation," in *Mathematics and Control in Smart Structures*, V.V. Varadan, Ed., 1998, vol. 3323 of *SPIE*, pp. 267–277.
- [11] G. Tao and P. V. Kokotović, "Adaptive control of plants with unknown hysteresis," *IEEE Transactions on Automatic Control*, vol. 40, no. 2, pp. 200–212, 1995.
- [12] G. V. Webb, D. C. Lagoudas, and A. J. Kurdila, "Hysteresis modeling of SMA actuators for control applications," *Journal of Intelligent Materials Systems and Structures*, vol. 9, no. 6, pp. 432–448, 1998.
- [13] K. Kuhnen and H. Janocha, "Adaptive inverse control of piezoelectric actuators with hysteresis operators," in *Proceedings of European Control Conference (ECC)*, Karlsruhe, Germany, 1999, Paper F 0291.
- [14] I. D. Mayergoyz, *Mathematical Models of Hysteresis*, Springer Verlag, 1991.
- [15] A. Visintin, *Differential Models of Hysteresis*, Springer, 1994.
- [16] X. Tan, *Control of Smart Actuators*, Ph.D. thesis, University of Maryland, College Park, MD, 2002, available as ISR Technical Report PhD 2002-8 at <http://techreports.isr.umd.edu/ARCHIVE>.
- [17] G. C. Goodwin and K. S. Sin, *Adaptive Filtering, Prediction and Control*, Prentice-Hall, Inc., Englewood Cliffs, NJ, 1984.
- [18] S. Sastry and M. Bodson, *Adaptive Control: Stability, Convergence, and Robustness*, Prentice Hall, Englewood Cliffs, NJ, 1989.